Reaction of Mercury(0) with the I_2 Adduct of Tetraphenyldithioimidodiphosphinic Acid $(SPPh_2)_2NH$ (HL) − Crystal Structures of $[Hg(HL)I_2]$ and HgL_2

M. Carla Aragoni,[a] Massimiliano Arca,[a] M. Bonaria Carrea,[a] Francesco Demartin,[b] Francesco A. Devillanova,[a] Alessandra Garau,[a] Francesco Isaia,*[a] Vito Lippolis,[a] and G. Verani[a]

Keywords: Bridging ligands / Coordination chemistry / Density functional calculations / Iodine / Mercury / S ligands

The complex $[Hg(HL)I_2]$ (**1**) has been synthesised by reacting liquid Hg(0) in Et_2O under mild reaction conditions with the I_2 adduct of HL, $HL{\cdot}I_2$, while HgL_2 (**2**) has been obtained from the reaction of compound **1** with HL in CH_3CN. A single-crystal X-ray investigation of **1** shows four independent molecules in the asymmetric unit, each of which contains an Hg^{II} ion coordinated to two iodine atoms and two sulfur atoms of one bidentate neutral ligand in a distorted tetrahedral coordination geometry. Compound **2** consists of two anionic ligands coordinated to an Hg^{II} ion, which again displays a distorted tetrahedral coordination sphere. The reaction of **2** with HI (55 wt.-% in water) affords $[Hg(HL)_2](I)_2$ (**3**). Compounds **1**, **2**, and **3** have been characterised by FT-IR and ^{31}P NMR spectroscopy. Density functional calculations suggest that compound **3** should feature a distorted tetrahedral coordination around the metal centre, with unequal Hg–S bond lengths.

Introduction

The oxidation/complexation reaction of metal powders by diiodine adducts of phosphane and polyfunctional thione donors has been investigated thoroughly in recent years. Numerous papers on this subject have shown this synthetic route to be a useful tool for obtaining coordination compounds with unusual geometries, stoichiometries, and oxidation numbers at the metal centre. In fact, owing to the majority use of $R_3E{\cdot}X_2$ adducts (R = alkyl, aryl; E = P, As, Sb; $X_2 = I_2$, Br_2, IBr), novel metal tertiary phosphane, arsane, and stibine complexes have been prepared by McAuliffe and co-workers.[1] Recently, another class of powerful oxidation reagents based on the I_2 and IBr adducts of *N*,*N*′-dimethylperhydrodiazepine-2,3-dithione has been employed successfully to oxidise gold metal in a one-step reaction under mild conditions. This reaction has found potential industrial applications in the fields of electronics and the recovery of precious metals from waste materials.[2]

Thanks to our extensive experience in the area of I_2 adducts of sulfur- and selenium-containing donors,[3] mainly aimed at improving our understanding of the nature of donor-I_2 bonding, we have recently decided to investigate the metal activation reaction by using tetraphenyldithioimidodiphosphinic acid $HN(Ph_2PS)_2$ (HL), which contains both group 15 and 16 elements, as the donor/complexing agent. Our choice was driven both by the donor ability of phosphane-sulfide compounds[4] towards I_2 and by the well-known intrinsic ability of L to give chelation and to favour the preferred geometry required by the metal ion.[5,6] Generally, the reaction of HL with metal ions leads to the formation of the anion L, which has the negative charge delocalised over the SPNPS moiety, and is capable of coordinating a metal centre through the two sulfur atoms, to form six-membered $MSSP_2N$ metallacycles.[5,6]

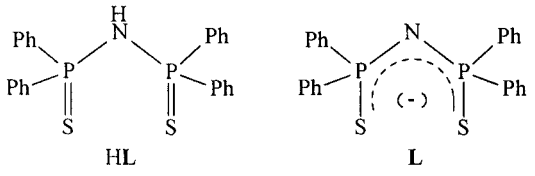

In this context, the I_2 adduct of HL, $HL{\cdot}I_2$, has shown an interesting potential in the oxidation/complexation of zerovalent metals in a low-polar solvent, as demonstrated by the results described above. Antimony(0) powder, for example, has been easily oxidised to Sb^{III} in a single step to give the unusual, X-ray characterised, dinuclear complex

[a] Dipartimento di Chimica Inorganica ed Analitica, Università di Cagliari,
S. S. 554 bivio per Sestu, 09042 Cagliari, Italy
E-mail: isaia@unica.it
[b] Dipartimento di Chimica Strutturale e Stereochimica Inorganica, Università di Milano,
Via G. Venezian 21, 20133 Milano, Italy

  DOI: 10.1002/ejic.200400279

[LSb(μ-S)(μ-I)$_2$SbL].[7] Similarly, the adduct HL·I_2 reacts with palladium and cobalt powders to produce the complexes PdL_2 [8] and CoL_2.[9]

Since there is a current interest in the chemistry of mercury, which stems from its widespread industrial use as well as its inherent toxicity and hazardous effects on human health,[10,11] and considering the promising results obtained with this synthetic route for other zero-valent metals, we report here on the reaction of HL·I_2 with liquid mercury with a view to opening new perspectives for the recovery of mercury(0) from industrial waste materials.[12]

Results and Discussion

Synthesis and X-ray Crystal-Structure Determination of [Hg(HL)I_2] and HgL_2

The reaction between equimolar quantities of the adduct HL·I_2 (generated in situ) and Hg ([HL·I_2] = 2.22 × 10^{-3} M, 25 °C) was carried out under nitrogen and anhydrous conditions in diethyl ether solution. The dark-red colour of the reaction mixture, due to the HL·I_2 charge-transfer adduct, disappeared almost completely within six hours with formation of an insoluble whitish precipitate. At this stage of the reaction, the concentration of HL·I_2 in the mixture is negligible, as determined from the very low intensity of the blue-shifted band of iodine[13] at 460 nm; moreover, no phosphorus-containing species was detectable by ^{31}P NMR spectroscopy. Elemental analysis of the separated solid and ^{31}P NMR spectroscopy confirmed the formation of [Hg(HL)I_2] (**1**) with the ligand in its neutral form. In this reaction, the zero-valent mercury is oxidised to Hg^{II} according to Equation (1).

$$Hg + HL{\cdot}I_2 \xrightarrow{Et_2O} Hg(HL)I_2 \quad (1)$$

Complexes containing metal ions coordinated to undissociated HL are very scarce in the literature since anything less than strictly anhydrous reaction conditions or the use of polar solvents always provokes imido-proton dissociation and the consequent formation of the deprotonated ligand L.[5a,6e] In this respect, in the case of the reactions with cobalt(0) and palladium(0) we were able to isolate the species [Co(HL)I_2] and [Pd(HL)I_2], but not to obtain suitable crystals since crystallization attempts always led to the formation of complexes CoL_2 [8] and PdL_2.[9]

The reaction in Equation (1) was also carried out in the presence of an excess of the adduct (1:2 Hg:HL·I_2 molar ratio) in order to synthesise complexes with a different stoichiometry. In addition to the formation of complex **1**, a small amount of white crystals of stoichiometry HgL_2 (**2**) was obtained after concentration of the reaction solution. Although complex **2** has been reported previously,[6e] its crystal structure has not been solved, and the complex has only partly been investigated. Moreover, since no structurally characterised complexes bearing HL have been reported in the literature, and due to the current interest in mercury complexes with dichalcogenoimidodiphosphinate derivatives,[14a−14c] we expanded our study on **1** and **2** by characterising the complexes by X-ray single-crystal diffractometry and ^{31}P NMR and FT-IR spectroscopy; DFT calculations on the simplified model complexes [Hg{N(H$_2$PS)$_2$}$_2$] and [Hg{HN(H$_2$PS)$_2$}$_2$I$_2$], and on the ion [Hg{HN(H$_2$PS)$_2$}$_2$]$^{2+}$ were carried out as well.

The X-ray structures of **1** and **2** are reported in Figure 1 and 2, respectively; selected bond lengths and angles are given in Table 1. The asymmetric unit of compound **1** contains four independent [Hg(HL)I_2] molecules with the metal centres labelled Hg(1), Hg(2), Hg(3), and Hg(4), respectively. Each molecule consists of an Hg^{II} ion coordinated to two iodide ions and one HL ligand, with the metal ion showing a very distorted tetrahedral coordination geometry [X−Hg−X angles (X = I, S) in the range 91.14(8)−135.66(4)°]. The HgSPNPS metallacycle displays a pseudo-boat conformation similar to that found in other metal complexes containing the anionic ligand L,[5] with a

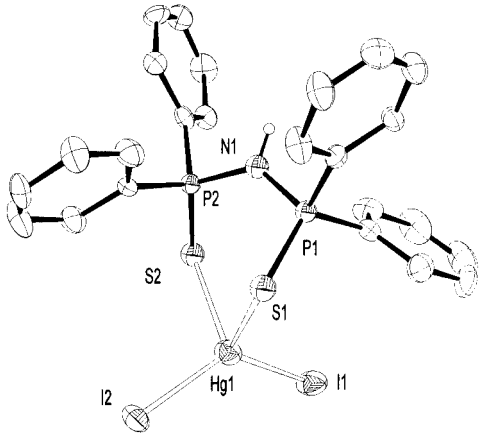

Figure 1. ORTEP plot of one of the crystallographically independent molecules of [Hg(HL)I_2] (**1**); thermal ellipsoids are shown at 50% probability; hydrogen atoms, except for the one bonded to the nitrogen, have been omitted for clarity

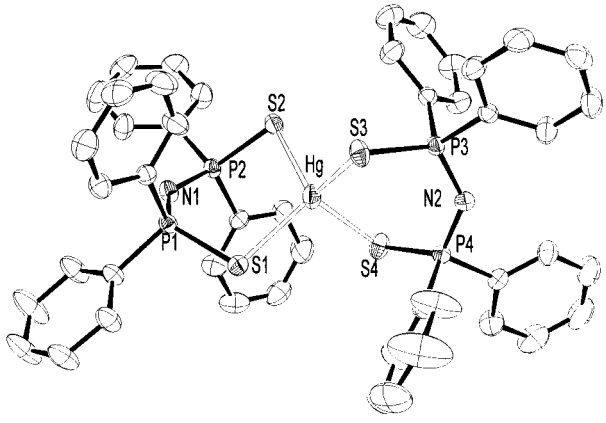

Figure 2. ORTEP plot of [Hg(L)$_2$] (**2**); thermal ellipsoids are depicted at 50% probability; hydrogen atoms have been omitted for clarity

Table 1. Selected interatomic distances (Å) and angles (°) in the structures of **1** and **2**

[Hg(HL)I$_2$] (**1**)			
Hg(1)−I(1)	2.662(1)	Hg(2)−I(3)	2.683(1)
Hg(1)−I(2)	2.691(1)	Hg(2)−I(4)	2.676(1)
Hg(1)−S(1)	2.692(3)	Hg(2)−S(3)	2.660(4)
Hg(1)−S(2)	2.709(3)	Hg(2)−S(4)	2.681(4)
S(1)−P(1)	1.960(4)	S(3)−P(3)	1.966(4)
S(2)−P(2)	1.970(4)	S(4)−P(4)	1.983(5)
P(1)−N(1)	1.674(9)	P(3)−N(2)	1.645(9)
P(2)−N(1)	1.686(9)	P(4)−N(2)	1.687(9)
Hg(3)−I(5)	2.681(1)	Hg(4)−I(7)	2.694(1)
Hg(3)−I(6)	2.678(1)	Hg(4)−I(8)	2.656(1)
Hg(3)−S(5)	2.665(4)	Hg(4)−S(7)	2.715(3)
Hg(3)−S(6)	2.679(4)	Hg(4)−S(8)	2.681(3)
S(5)−P(5)	1.964(5)	S(7)−P(7)	1.962(4)
S(6)−P(6)	1.980(5)	S(8)−P(8)	1.969(4)
P(5)−N(3)	1.650(9)	P(7)−N(4)	1.659(9)
P(6)−N(3)	1.691(10)	P(8)−N(4)	1.672(9)
I(1)−Hg(1)−S(1)	118.79(8)	S(5)−Hg(3)−I(6)	118.46(9)
I(1)−Hg(1)−I(2)	134.00(3)	S(5)−Hg(3)−S(6)	96.96(10)
S(1)−Hg(1)−I(2)	91.45(8)	I(6)−Hg(3)−S(6)	95.24(8)
I(1)−Hg(1)−S(2)	95.07(8)	S(5)−Hg(3)−I(5)	94.55(7)
S(1)−Hg(1)−S(2)	96.27(9)	I(6)−Hg(3)−I(5)	128.49(5)
I(2)−Hg(1)−S(2)	116.54(8)	S(6)−Hg(3)−I(5)	120.29(9)
S(3)−Hg(2)−I(4)	117.32(9)	I(8)−Hg(4)−S(8)	117.43(8)
S(3)−Hg(2)−S(4)	97.31(11)	I(8)−Hg(4)−I(7)	135.66(4)
I(4)−Hg(2)−S(4)	95.65(9)	S(8)−Hg(4)−I(7)	91.14(8)
S(3)−Hg(2)−I(3)	95.45(8)	I(8)−Hg(4)−S(7)	96.17(8)
I(4)−Hg(2)−I(3)	129.42(5)	S(8)−Hg(4)−S(7)	95.87(9)
S(4)−Hg(2)−I(3)	118.43(9)	I(7)−Hg(4)−S(7)	114.92(8)
HgL$_2$ (**2**)			
Hg−S(1)	2.5167(8)	S(1)−P(1)	2.0221(9)
Hg−S(2)	2.5436(7)	S(2)−P(2)	2.0221(9)
Hg−S(3)	2.5430(7)	S(3)−P(3)	2.0157(9)
Hg−S(4)	2.5569(8)	S(4)−P(4)	2.0135(9)
P(1)−N(1)	1.587(2)	P(3)−N(2)	1.590(2)
P(2)−N(1)	1.583(2)	P(4)−N(2)	1.585(2)
S(1)−Hg−S(2)	112.13(2)	S(2)−Hg−S(3)	111.44(3)
S(1)−Hg−S(3)	108.93(3)	S(2)−Hg−S(4)	104.42(3)
S(1)−Hg−S(4)	108.30(3)	S(3)−Hg−S(4)	111.54(2)

P and an S atom of the ring acting as the stern and bow of the boat. Two out of the four independent complex molecules, Hg(2) and Hg(3), conform to an almost exact C_2 symmetry, the twofold axis passing through the Hg and N atoms and the puckering of the HgSPNPS metallacycle having the same absolute configuration. As regards the other two [those containing Hg(1) and Hg(4)] the conformation of the ring is much more distorted and the absolute configuration is the opposite of that found in the former two complex molecules (see Figure 3a and 3b). Such distortions, together with some variability in the length of chemically equivalent interactions, are due to packing effects, which play an important role in determining the actual symmetry of the crystal. The P−S distances are, on average, only slightly, although significantly, longer than those found in the uncoordinated ligand HL[15] [1.969(5) vs. 1.937(1)−1.959(1) Å]. Conversely, no significant variation is detected for the P−N bonds [average 1.670(9) vs. 1.672(2)−1.683(2) Å].

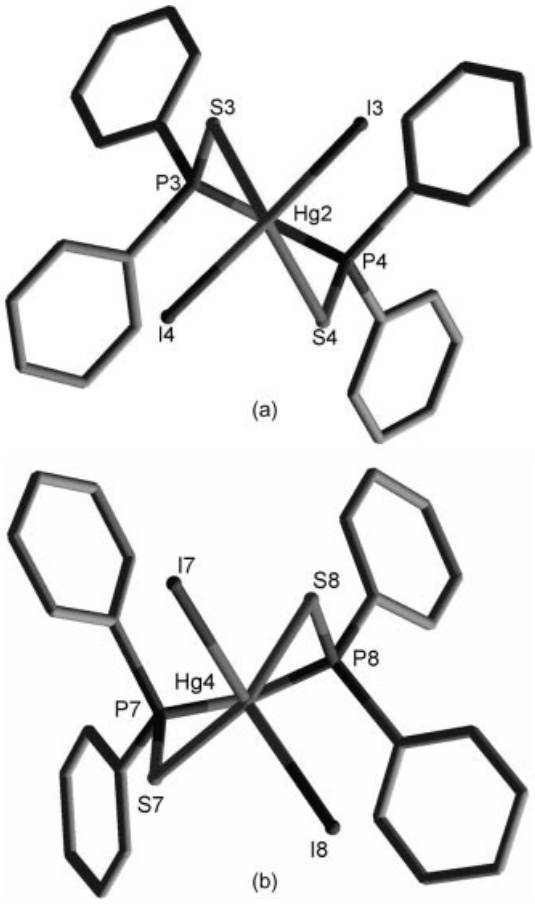

Figure 3. View along the axis connecting Hg(2)−N(2) (a) and Hg(4)−N(4) (b) in complex **1**

Compound **2** consists of two anionic L ligands coordinated to an Hg^{II} ion, which displays tetrahedral coordination geometry. Distortion from the idealized tetrahedral geometry is less pronounced than in complex **1**, the S−Hg−S angles ranging from 104.42(3)° to 112.13(2)°. Each of the two pseudo-boat metallacycles arising from coordination of the anionic ligand to the metal ion displays an almost exact C_2 symmetry, with the twofold axis joining the metal and the N atoms. However, the two rings have opposite configurations within the same molecule. As a result of deprotonation and coordination, the P−S distances increase from 1.937(1)−1.950(1) Å in the free ligand to 2.0135(9)−2.0221(9) Å in **2** and, accordingly, the P−N bond lengths decrease from 1.672(2)−1.683(2) to 1.583(2)−1.590(2) Å.

Complexes **1** and **2** are easily distinguishable by IR spectroscopy since, upon coordination, HL and L have a different π-electron delocalisation over the chelating ring HgSPNPS. The ν_{asym}(PNP) stretching band, which is the most sensitive to metal coordination,[6e] occurs in HL as a strong absorption at 922 cm^{-1}; this increases by about 300 cm^{-1} when the imido proton is removed. As regards the ν(P−S) stretching frequencies, a 30−60 cm^{-1} and 50−80 cm^{-1} decrease is expected upon metal-ion chelation of HL and L, respectively. The IR spectra of **1** and **2** support these findings: the ν(P−S) stretching frequencies measured in

complex **1** (606 and 592 cm^{-1}) and in complex **2** (576 and 561 cm^{-1}) agree with a lower P−S bond order than the free ligand HL (645 and 622 cm^{-1} for the antisymmetric and symmetric stretching modes, respectively);[6d,6e] the ν_{asym}(PNP) stretching frequency (922 cm^{-1} in HL)[6d,6e] appears at 916 cm^{-1} in **1** and 1239 and 1219 cm^{-1} in **2**; these values are within the expected frequency range for single-bonded P−N and double-bonded P=N stretching regions, respectively.

The ^{31}P CP MAS NMR spectrum of complex **1** shows the presence of a single broad resonance at δ = 59.5 ppm with a spectral line-width of 300 Hz, suggesting that the eight phosphorus atoms in the asymmetric unit have a very similar environment. Conversely, the ^{31}P CP MAS NMR spectrum of **2** shows the presence of three resonances at δ = 40.0 ($\Delta\nu_{1/2}$ = 155 Hz), 37.8 ($\Delta\nu_{1/2}$ = 163 Hz), and 33.9 ppm ($\Delta\nu_{1/2}$ = 148 Hz), with a relative intensity ratio of approximately 1:1:2. Evidently, small bond-length differences in the anionic ligands L imply a different charge distribution over the SPNPS fragment and lead to a significant effect on the phosphorus chemical shifts. This effect is not observed for complex **1**, where the neutral ligand HL is involved in the metal coordination. The ^{31}P NMR spectrum (in CH_2Cl_2) of **1** exhibits a single resonance at δ = 57.8 ppm ($\Delta\nu_{1/2}$ = 8.1 Hz), which confirms the presence of the ligand in the complex in its neutral form when in solution too, since deprotonation/complexation of the ligand results in a high-field shift of the ^{31}P NMR signal of about 20−30 ppm. The corresponding chemical shift for HL in the same solvent is δ = 56.6 ppm ($\Delta\nu_{1/2}$ = 3.6 Hz), and the small change caused by coordination is in keeping with the structural similarities between the free and bound ligand in the solid state. The absence of any Hg/P coupling suggests that, at room temperature, the ligand HL is labile on the NMR timescale. In fact, as increasing amounts of HL are added to the solution of the complex up to a 3:1 molar ratio, only one phosphorus resonance is observed, although the chemical shift decreases towards the value of δ = 56.6 ppm as a consequence of the weighted average of the individual shifts of the contributing species **1** and free HL. Low-temperature measurements were carried out to as low as −70 °C, the lowest temperature for which ^{31}P NMR spectroscopic data were recordable, with no Hg/P coupling or significant shifts in the position of the resonance being observed. The broadening of the signal with decreasing temperature (25 °C, $\Delta\nu_{1/2}$ = 8.1 Hz; −70 °C, $\Delta\nu_{1/2}$ = 10.4 Hz) is indicative of the expected slowing of the chemical-exchange process. Obviously, we were not able to achieve the temperature at which the complex is "frozen out" on the NMR timescale.

In the case of complex **2**, the ^{31}P NMR spectrum (CH_2Cl_2) shows only one resonance at δ = 39.7 ppm ($\Delta\nu_{1/2}$ = 6 Hz) flanked by mercury satellites with a $^2J_{(^{199}Hg-^{31}P)}$ coupling of 101 Hz. Thus, in solution at room temperature, unlike the situation found in the solid state, the four phosphorus atoms in the complex are equivalent, indicating that the three resonances found in the solid state are due to solid-state effects. Addition of an equimolar amount of HL to a solution of **2** ([**2**] = 1.1 × 10^{-2} M; CH_2Cl_2, 25 °C) gives a ^{31}P NMR spectrum with two resonances, one due to the free ligand and one due to the complex. Variable-temperature NMR experiments were carried out to as low as −80 °C, the lowest temperature for which ^{31}P NMR spectroscopic data were recordable, with no significant change in the spectra, suggesting the presence of different conformers.

Reaction Chemistry of $[Hg(HL)I_2]$ and HgL_2

The attempts to synthesise new complexes by reacting $[Hg(HL)I_2]$ (**1**) with increasing amounts of HL proved unsuccessful ([**1**] = 2.5 × 10^{-3} M; HL to **1** molar ratio 3:1; CH_2Cl_2, 25 °C). However, the same reaction carried out in a more polar solvent like CH_3CN (HL to **1** molar ratio 1:1; 25 °C) leads to the quantitative formation of complex **2**, thus confirming that in polar solvents HL is prone to lose the imido proton when complexed to a metal.[6e,8,9]

The reaction of complex **1** with hydroiodic acid (55 wt.-% in water) was also evaluated since it may prove useful in freeing the ligand from the complex. Examination of the equimolar reaction between HI and compound **1** (CH_2Cl_2, 25 °C) by ^{31}P NMR spectroscopy revealed only one signal at δ = 57.3 ppm, which is only slightly high-field shifted with respect to the resonance of complex **1**; conversely, when a twentyfold excess of HI is employed the resonance is found at δ = 56.6 ppm, indicating the presence of free HL in the solution [Equation (2)]. Raman spectra carried out on the organic phase confirmed the presence of free HL, whereas in the water phase a peak at 121 cm^{-1} is indicative of the formation of the anion $[HgI_4]^{2-}$.[16]

$$Hg(HL)I_2 + 2HI(aq) \xrightarrow{CH_2Cl_2} HL + 2H^+(aq) + HgI_4^{2-}(aq) \quad (2)$$

Equation (1) and (2) could obviously be very important as far as a recovery process is concerned, since they allow not only an easy oxidation of mercury(0) to mercury(II), but also the possibility to free the metal from the complex **1** and to recover the ligand HL.

Reaction of **2** with hydroiodic acid (55 wt.-% in water) in a 1:2 molar ratio in CH_2Cl_2 results in a considerable change in the ^{31}P NMR spectrum of the complex (Figure 4a and 4b). Indeed, the signal of **2** at δ = 39.5 ppm disappears completely and a new signal is observed at low field (δ = 57.6 ppm). The shift of the signal and its value, which is similar to that of complex **1** (δ = 57.8 ppm, CH_2Cl_2), strongly indicate the successful protonation of the anionic ligand in the complex. Slow concentration of the dichloromethane solution afforded a white powder, whose microanalysis suggests a stoichiometry $[Hg(HL)_2](I)_2$ (**3**). The ^{31}P CP MAS NMR spectrum of **3** shows a broad band at δ = 59.1 ppm ($\Delta\nu_{1/2}$ = 494 Hz), confirming the presence of the ligands in their neutral form in the complex. IR bands at 565 cm^{-1} [ν(P−S)], 922 cm^{-1} [ν(P−N)], and 2631 cm^{-1}, which originates from the first overtone of the δ(N−H) bending vibration[6e] at 1325 cm^{-1}, further support coordination of HL to the metal in **3**. In addition, the molar con-

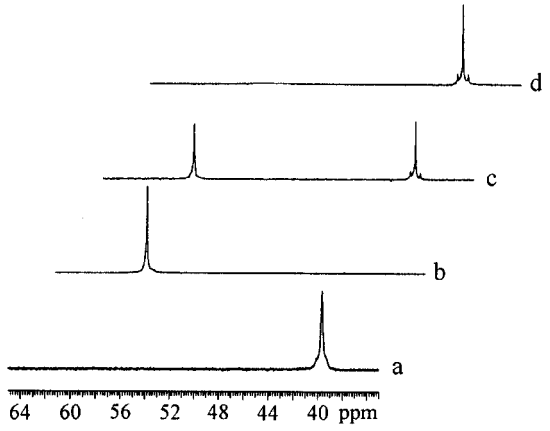

Figure 4. ^{31}P NMR spectra in CH_2Cl_2 (25 °C) of: (a) **2** (3.58×10^{-3} M); (b) solution of **2** after addition of HI (55 wt.-% in H_2O; **2**/HI 1:2 molar ratio); (c) the solution from (b) after addition of DMAN (**2**/HI/DMAN 1:2:1 molar ratio); (d) the solution from (c) after addition of more DMAN (**2**/HI/DMAN 1:2:2 molar ratio)

ductivity of **3** (660 $\mu S \cdot cm^2 \cdot mol^{-1}$, CH_2Cl_2, 25 °C) is considerably higher than that of **2** (93 $\mu S \cdot cm^2 \cdot mol^{-1}$, CH_2Cl_2, 25 °C). The protonation reaction is reversibl. A very strong base such as 1,8-bis(dimethylamino)naphthalene (DMAN) was added to a solution of **3** in CH_2Cl_2 in order to obtain 1:1 and 1:2 molar ratios of complex **3**/DMAN. In the former case the neutral complex **2** is partly regenerated (Figure 4c) and in the latter fully regenerated (see d in Figure 4), as shown by the ^{31}P NMR peak at $\delta = 39.5$ ppm. The reactions involving complexes **2** and **3** in CH_2Cl_2 are summarised in Scheme 1.

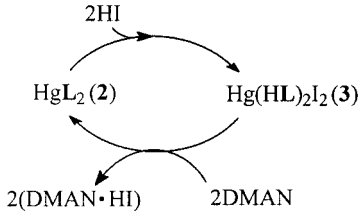

Scheme 1

Quantum-Chemical Calculations

In the light of the novelty of complex **1**, and in order to provide further insight into the electronic properties of the title compounds, we performed hybrid-DFT calculations on complexes **1** and **2**. We also determined the geometrical features of complex **3**. Theoretical calculations were performed on the model complexes $[Hg\{N(H_2PS)_2\}_2]$ (**4**) and $[Hg\{HN(H_2PS)_2(I)_2\}]$ (**5**), in which the phenyl groups have been replaced by hydrogen atoms, and subsequently on the model complex $[Hg\{HN(H_2PS)_2\}_2]^{2+}$ (**6**). As previously reported by us for similar model complexes, hybrid-DFT calculations have given reliable results in understanding both the structural and electronic features of the model complexes $[Pd\{N(H_2PS)_2\}_2]$[8] (**7**) and $[In\{N(H_2PS)_2\}I_2]$[9b] (**8**). Encouraged by our recent results,[17] the mPW1PW[18] functional was preferred to the B3LYP functional,[19] which was previously employed for **7** and **8**. As regards the ligand atoms, the pVDZ basis set of Schafer et al.[20,21] was used. The basis set for the metal atom is more difficult to choose since, due to the high atomic number of mercury, relativistic effects have to be taken into account. Thus, for **4** and **5**, we used the SBKJC with effective core potentials (ECP),[21,22] since the LanL2DZ basis set previously used successfully for Pd and In in **7** and **8** is not available for Hg. Geometry optimizations on **4** and **5**, performed starting from the structural data of **2** and **1**, respectively, show a very good agreement with the experimental data. Thus, in both complexes, the central mercury atom is coordinated by the ligand donor atoms in a distorted tetrahedral arrangement with average Hg−S bond lengths of 2.611 Å (experimental 2.543 Å).[23] Analogously, in the case of **5**, the average Hg−S and Hg−I bond lengths (2.889 and 2.743 Å, respectively) are very close to the experimental values determined for **1** (2.700 and 2.688 Å, respectively). In agreement with the experimental structures of **1** and **2**, a comparison of the optimized structural features of the ligand moiety in **4** and **5** shows that, upon protonation, we obtain a lengthening of the P−N bond lengths (1.606 and 1.709 Å in **4** and **5**, respectively) and a shortening of the P−S bond lengths (2.031 and 1.959 Å in **4** and **5**, respectively). In order to better understand the interaction between the metal ion and the ligands, a qualitative interpretation can be obtained from the fragment molecular orbital approach (FMO) within the formalism of the extended Hückel theory (EHT).[24] The interaction diagram between the 6s and 6p atomic orbitals of the Hg^{2+} ion and those of the ligands is shown in Figure 5, calculated at the DFT-optimised geometries. For both **4** and **5**, the Kohn−Sham HOMOs are nonbonding orbitals built from the p atomic orbitals of the donor atoms with a small contribution from the filled $5d_{xy}$ and $5d_{xz}$ orbitals of the central metal atom. The LUMOs are nonbonding in nature and they are made up of a combination of the 6s atomic orbital of the Hg ion σ-interacting with the p-orbitals of the donor atoms pointing towards the central metal ion. Confident in the agreement between the calculated geometries of **4** and **5** and their parent complexes, we extended our DFT calculations at the same level of theory to **6** so as to acquire information on the geometrical features of the parent cationic complex **3**. In this case the Hg ion is also coordinated by the two ligand units in a distorted tetrahedral fashion. In agreement with what emerges from the comparison of the calculated structural features of **4** and **5**, upon imido protonation, model **6** shows an increase in the Hg−S (average value 2.628 Å) and the P−N (average value 1.698 Å) bond lengths compared to those calculated for **4**, while the P−S bond lengths are slightly shortened (average value 1.993 Å). Since **4** and **6** are isoelectronic, their frontier orbitals are very similar in shape and composition. In particular, the Kohn−Sham HOMOs of **4** and **6** (see a in Figure 6) are slightly antibonding orbitals built from the p atomic orbitals of the donor atoms with a small contribution from the filled $5d_{xy}$ and $5d_{xz}$ orbitals of the central metal atom. On the other hand, in the case of **5** (c in Figure 5), the HOMO and the HOMO−1 are almost entirely centered on the iodides, and

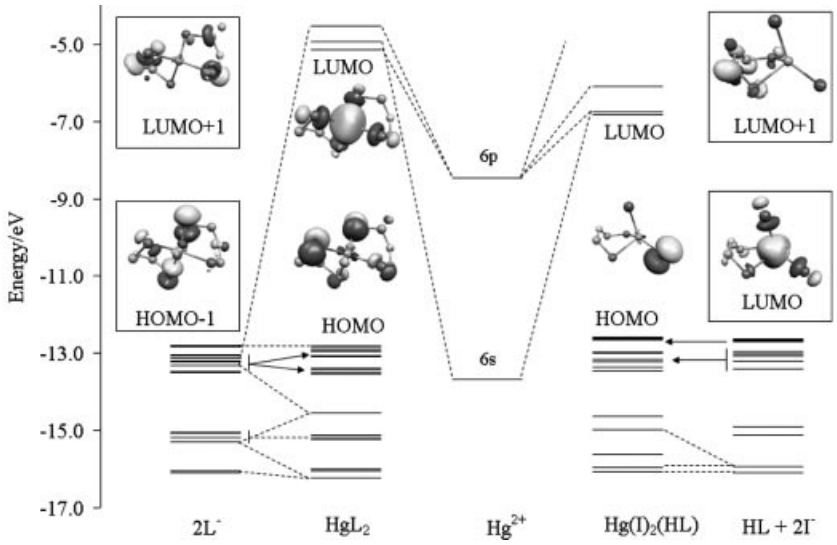

Figure 5. EHT-interaction diagram showing the interaction between the empty atomic orbitals of the Hg^{2+} central ion and the filled ones of the ligands HL in the model complexes **4** and **5** [HL = $H_2P(S)-NH-P(S)H_2$]; the dashed lines connect FMOs which contribute at least 15% to the formation of molecular orbitals; the hybrid-DFT frontier orbitals are also depicted (contour value 0.05)

they are therefore nonbonding in nature. The LUMOs of the three complexes are all antibonding in nature, and are due to the combination of the 6s atomic orbitals of the Hg ion σ-interacting with the p-orbitals of the donor atoms pointing towards the central metal ion (see b and d in Figure 5 for **4** and **5**, respectively).

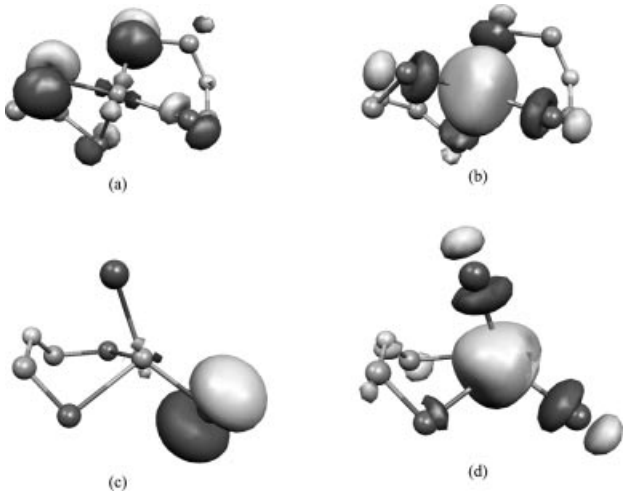

Figure 6. Sketches of Kohn−Sham HOMOs and LUMOs calculated for **4** (a and b, respectively), and **5** (c and d, respectively)

Conclusion

The oxidizing ability of the adduct $HL{\cdot}I_2$ in Et_2O towards liquid Hg(0) leads to the synthesis of the air stable complex $[Hg(HL)I_2]$ (**1**) in a single oxidation step. To the best of our knowledge, this complex represents the first example of a structurally characterised complex of HL. The reaction of **1** with an excess of HL in MeCN affords the neutral air stable complex $[Hg(L)_2]$ (**2**), which can also be obtained from the reaction of HgX_2 (X = Br, I) with HL. The reaction of **2** with concentrated HI leads to the species $[Hg(HL)_2](I)_2$ (**3**; see Scheme 2). X-ray diffraction analyses and DFT calculations on simplified model complexes have been performed to elucidate the structural and electronic properties of **3**. Complex **1** readily reacts with an excess of HI to yield the anion $[HgI_4]^{2-}$ with the release of HL, which can be re-utilised, hopefully opening new perspectives for the recovery of Hg(0) from mercury-containing waste materials.

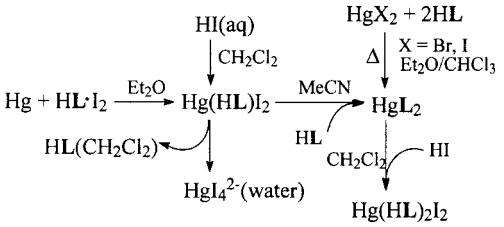

Scheme 2

Experimental Section

Materials and Instrumentation: All reagents were used as purchased from Aldrich. Diethyl ether was distilled from over $LiAlH_4$ shortly before use. CH_2Cl_2 was distilled from P_2O_5 and stored under N_2. All reactions were carried out under an atmosphere of dry nitrogen. $^{31}P\{^1H\}$ NMR spectra were recorded on a Varian Unity Inova 400 MHz operating at 161.9 MHz. The ^{31}P chemical shifts are referenced to an external standard of 85% H_3PO_4 (δ = 0.0 ppm). ^{31}P NMR CP MAS NMR spectra were calibrated indirectly from the H_3PO_4 peak (δ = 0.0 ppm). Variable temperature ^{31}P NMR spectroscopic data on compound **1** were collected from a 1.1×10^{-2} M solution in CH_2Cl_2 [temp. (°C), δ, $\Delta\nu_{1/2}$: 25, 57.7, 8.1; 0, 57.9, 8.6; −20, 58.1, 10.0; −40, 58.3, 10.2; −60, 58.3, 10.5, −70, 58.4, 10.4]. ^{31}P NMR data for compound **2** were collected from a 1.2×10^{-2} M solution in CH_2Cl_2 [temp. (°C), δ, $\Delta\nu_{1/2}$: 25, 39.5, 6.1; −20, 39.5,

9.0; −40, 39.5, 9.5; −70, 39.1, 12.9, −80, 39.2, 14.0]. IR spectra were measured as KBr (4000−400 cm^{-1}) or polyethylene pellets (400−50 cm^{-1}) on a Bruker IFS 55 FT-IR spectrometer. FT Raman spectra were recorded on a Bruker FRS 100 Fourier-transform Raman spectrometer, operating with a diode-pumped Nd:YAG exciting laser at 1064 nm. Conductometric measurements were carried out at 25 °C.

Synthesis: HL was prepared according to ref. 25. The adduct $HL{\cdot}I_2$ was prepared in situ in distilled Et_2O just before use from equimolar amounts of HL and I_2.

[Hg(HL)I$_2$] (1): A mixture of HL (0.100 g, 0.222 mmol) and I_2 (0.0565 g, 0.223 mmol) in Et_2O (100 mL) was stirred at room temperature under N_2 until complete dissolution of the reagents. Liquid mercury (0.0236 g, 0.222 mmol) was then added while stirring. This reaction was continued at room temperature under N_2 for about one day. The resulting air-stable whitish solid was isolated by suction filtration, washed with diethyl ether, and dried in vacuo, to give 0.172 g of **1** (0.211 mmol; yield 95%). Stable colourless crystals were obtained upon dissolution of **1** in anhydrous CH_2Cl_2 and subsequent slow evaporation of the solvent. $C_{24}H_{21}HgI_2NP_2S_2$ (903.87): calcd. C 31.89, H 2.34, N 1.55, S 7.09; found C 32.0, H 2.5, N 1.6, S 7.4. IR (KBr): $\tilde{\nu}$ = 3054w cm^{-1}, 2966w, 2924w, 2855w, 2606brw, 1435vs, 1384m, 1303m, 1184m, 1107vs, 916s, 804m, 782s, 733vs, 720vs, 685vs, 622w, 606ms, 592s, 506m, 487m, 464m, 441w. ^{31}P NMR (CH_2Cl_2): δ = 57.8 ppm. M.p. 228−230 °C (dec.).

[Hg(L)$_2$] (2). Method a: A mixture of HL (0.100 g, 0.222 mmol) and [Hg(HL)I_2] (0.200 g, 0.222 mmol) in CH_3CN (100 mL) was stirred at room temperature for 4 h. The solid white product was collected by filtration and then dissolved in hot CH_2Cl_2. The resulting solution was allowed to evaporate in air to yield a white solid. Yield: 0.230 g (0.210 mmol, 95%). **Method b:**[6e] A solution of HL (0.125 g, 2.774. mmol) in $CHCl_3$ (10 mL) was added to a solution of $HgBr_2$ (0.050 g, 1.387 mmol) in Et_2O (10 mL). The reaction mixture was stirred for 1 h at room temperature and then refluxed for 20 min. The solid product was separated by filtration, washed twice with a 1:1 acetone/diethyl ether mixture, and dried under vacuum to give 0.136 g of **2** (89% yield). $C_{48}H_{40}HgN_2P_4S_4$ (1097.5): calcd. C 52.32, H 3.67, N 2.55, S 11.68; found C 53.0, H 3.9, N 2.6, S 12.0. IR (KBr): $\tilde{\nu}$ = 3054m cm^{-1}, 2918w, 2846w, 1475w, 1436s, 1384w, 1239s, 1219s, 1174s, 1103s, 1025w, 997w, 786w, 742m, 714s, 698vs, 618w, 576s, 561vs, 514s, 495m. ^{31}P NMR (CH_2Cl_2): δ = 39.7 ppm. M.p. > 255 °C

[Hg(HL)$_2$](I)$_2$ (3): A dichloromethane solution (10 mL) of **2** (0.020 g, 0.018 mmol) and a hydroiodic acid solution (55 wt.-% in water; 0.0092 g, 0.04 mmol) were vigorously stirred for 1 h at 25 °C. The colourless two-phase mixture was then passed through a phase-separation filter (Whatman, Phase Separator 1PS) to remove the water. After concentration of the solution to about 5 mL, *n*-hexane (5 mL) was added dropwise and a white solid precipitated. This was washed with *n*-hexane and dried to give 0.018 g of **3** (74% yield). $C_{48}H_{42}HgI_2N_2P_4S_4$ (1353.4): calcd. C 42.60, H 3.13, N 2.07, S 9.48; found C 43.0, H 3.2; N 2.2, S 10.0. IR (KBr): $\tilde{\nu}$ = 2631w cm^{-1}, 1436vs, 1325m, 1218m, 1106s, 922s, 785s, 741s, 716s, 688vs, 649m, 561s, 513m. ^{31}P NMR (CH_2Cl_2): δ = 57.6 ppm. M.p. 203−204 °C

X-ray Crystallography: Crystal data and refinement details for structure determinations of both compounds are reported in Table 2. Intensity data were acquired at room temperature on a SMART CCD diffractometer (ω scans). All data sets were corrected for Lorentz-polarisation effects and for absorption using the SADABS routine.[26] The structures were solved by direct methods using the SHELXS 97 program,[27] followed by difference Fourier synthesis, and refined by full-matrix least-squares procedures on F^2 using the SHELXL-97 program.[28] All non-H atoms were refined anisotropically and H atoms were introduced at calculated positions and thereafter incorporated into a riding model with $U_{iso}(H) = 1.2U_{eq}(C)$. For compound **1** the search for an alternative symmetry other than the triclinic one reported in Table 2 was done using Le Page's MISSYM (PLATON) routine.[29] The check revealed that the triclinic unit cell can be transformed metrically into an almost-monoclinic C-centred unit cell with a = 24.485(3), b = 24.506(3), c = 19.230(3) Å, α = 90.42(1), β = 103.25(1), γ = 89.61(1)°. However, with this choice, the agreement between equivalent reflections was poor (R_{int} = 0.434) thus ruling out the possibility of the symmetry being monoclinic.
CCDC-228871 (for **1**) and -228872 (for **2**) contain the supplementary crystallographic data for this paper. These data can be obtained free of charge at www.ccdc.cam.ac.uk/conts/retrieving.html [or from the Cambridge Crystallographic Data Centre, 12 Union Road, Cambridge CB2 1EZ, UK; Fax: +44-1223-336033; E-mail: deposit@ccdc.cam.ac.uk].

Table 2. Crystal data and details of refinements for [Hg(HL)I_2] and HgL_2

Compound	[Hg(HL)I_2] (**1**)	HgL_2 (**2**)
Formula	$C_{24}H_{21}HgI_2NP_2S_2$	$C_{48}H_{40}HgN_2P_4S_4$
Mol. mass (amu)	903.87	1097.53
Crystal system	triclinic	triclinic
Space group	$P\bar{1}$ (no. 2)	$P\bar{1}$ (no. 2)
a (Å)	17.262(2)	13.626(1)
b (Å)	17.380(2)	13.794(1)
c (Å)	19.230(3)	14.336(1)
α (°)	99.59(1)	82.21(1)
β (°)	99.05(1)	66.10(1)
γ (°)	90.05(1)	69.44(1)
U (Å^3)	5616(1)	2306.6(4)
Z	8	2
ρ_{calcd} (Mg·m^{-3})	2.138	1.580
μ(Mo-K_α) (mm^{-1})	7.957	3.692
Transmission factors	0.602−1.000	0.735−1.000
Unique refl. with $I > 2\sigma(I)$	9240	8871
Final R and $wR2$ indices	0.0496, 0.1225	0.0243, 0.0613

Computations: Quantum-chemical DFT calculations were carried out with the Gaussian 98 (rev. A11)[30] suite of programs on the model complexes [Hg{N($H_2PS)_2$}$_2$] (**4**), [Hg{N($H_2PS)_2$}I_2] (**5**), and [Hg{HN($H_2PS)_2$}$_2$]$^{2+}$ (**6**), with Adamo and Barone's mPW1PW functional[18] and pVDZ Schafer, Horn and Ahlrichs pVDZ basis sets for H, N, P, and S.[20,21] For Hg and I, the SBKJC basis set with effective core potentials was used.[22] In the case of **4**, the calculations were also performed with the Stuttgart RLC ECP basis set for Hg.[23] Integration was performed numerically using a total of 7500 points for each atom (Finegrid option). The geometry optimizations of **4**, **6** and **5** were performed starting from the experimental geometries determined for **1** and **2**, avoiding introducing any symmetry constraint. DFT calculations were performed on an SGI Origin 3800 equipped with 128 GByte of RAM. The results of the calculations were analysed with the Molekel 4.3[32a] and Molden 3.9[32b] programs. The quantum mechanically optimised structure was verified by normal-mode harmonic frequency analysis. Harmonic frequencies were obtained using the second derivatives of the DFT energy, computed by numerical differentiation of the DFT energy gradients. The qualitative EHT analyses were obtained with the CACAO (Computer Aided Composition of

Atomic Orbitals) program package[32c] on the hybrid-DFT-optimised geometry. The interaction diagram was generated using the fragment molecular orbital (FMO) approach.[32d] Parameters used in EHT calculations were taken from the standard database of CACAO.

Acknowledgments

This research was financially supported by the "Regione Autonoma della Sardegna". We are grateful to CINECA (Consorzio Interuniversitario per il Calcolo Automatico dell'Italia Nord Orientale) for providing computational facilities.

[1] [1a] S. M. Godfrey, C. A. McAuliffe, R. G. Pritchard, J. M. Sheffield, *Inorg. Chim. Acta* **1999**, *292*, 213−219. [1b] S. M. Godfrey, N. Ho, C. A. McAuliffe, R. G. Pritchard, *Angew. Chem. Int. Ed. Engl.* **1996**, *33*, 2344−2345. [1c] C. A. McAuliffe, S. M. Godfrey, A. G. Mackie, R. G. Pritchard, *Angew. Chem. Int. Ed. Engl.* **1992**, *31*, 919−921, and references cited therein.

[2] [2a] L. Cau, P. Deplano, L. Marchiò, M. L. Mercuri, L. Pilia, A. Serpe, E. F. Trogu, *Dalton Trans.* **2003**, 1969−1974. [2b] F. Bigoli, P. Deplano, M. L. Mercuri, M. A. Pellinghelli, G. Pintus, A. Serpe, E. F. Trogu, *J. Am. Chem. Soc.* **2001**, *123*, 1788−1789. [2c] F. Bigoli, P. Deplano, M. L Mercuri, M. A. Pellinghelli, G. Pintus, M. A. Serpe, E. F. Trogu, *Chem. Commun.* **1998**, 2351−2352. [2d] F. Bigoli, P. Deplano, F. A. Devillanova, V. Lippolis, M. L. Mercuri, M. A. Pellinghelli, E. F. Trogu, *Inorg. Chim. Acta* **1998**, *267*, 115−121.

[3] [3a] M. C. Aragoni, M. Arca, F. Demartin, F. A. Devillanova, A. Garau, F. Isaia, V. Lippolis, G. Verani, *Trends Inorg. Chem.* **1999**, *6*, 1−18. [3b] M. C. Aragoni, M. Arca, F. Demartin, F. A. Devillanova, A. Garau, F. Isaia, V. Lippolis, G. Verani, *Coord. Chem. Rev.* **1999**, *184*, 271−290. [3c] M. C. Aragoni, M. Arca, A. J. Blake, F. A. Devillanova, W.-W. du Mont, A. Garau, F. Isaia, V. Lippolis, G. Verani, C. Wilson, *Angew. Chem. Int. Ed.* **2001**, *40*, 4229−4232.

[4] [4a] M. Arca, F. A. Devillanova, A. Garau, F. Isaia, V. Lippolis, G. Verani, F. Demartin, *Z. Anorg. Allg. Chem.* **1998**, *624*, 745−749. [4b] M. Arca, F. Demartin, F. A. Devillanova, A. Garau, F. Isaia, V. Lippolis, G. Verani, *J. Chem. Soc., Dalton Trans.* **1999**, 3069−3073.

[5] [5a] I. Haiduc, *Comprehensive Coordination Chemistry II*, vol 1 (Ed.: A. B. P. Lever), Elsevier Pergamon, Amsterdam, Oxford, **2004**, p. 323−347. [5b]C. Silvestru, J. E. Drake, *Coord. Chem. Rev.* **2001**, *223*, 117−216. [5c] T. Q. Ly, J. D. Woollins, *Coord. Chem. Rev.* **1998**, *176*, 451−481, and references cited therein.

[6] [6a] C. G. Pernin, J. A. Ibers, *Inorg. Chem.* **2000**, *39*, 1216−121. [6b] C. G. Pernin, J. A. Ibers, *Inorg. Chem.* **2000**, *39*, 1222−1226. [6c] O. Siiman, C. P. Huber, M. L. Post, *Inorg. Chim. Acta* **1977**, *25*, L11−L14. [6d] O. Siiman, J. Vetuskey, *Inorg. Chem.* **1980**, *19*, 1672−1680. [6e] G. P. McQuillan, I. A. Oxton, *Inorg. Chim. Acta* **1978**, *29*, 69−75.

[7] M. Arca, F. A. Devillanova, A. Garau, F. Isaia, V. Lippolis, G. Verani, G. L. Abbati, A. Cornia, *Z. Anorg. Allg. Chem.* **1999**, *625*, 517−520.

[8] G. L. Abbati, M. C. Aragoni, M. Arca, A. C. Fabretti, F. A. Devillanova, A. Garau, F. Isaia, V. Lippolis, G. Verani, *J. Chem. Soc., Dalton Trans.* **2001**, 1105−1110.

[9] [9a] M. C. Aragoni, M. Arca, A. Garau, F. Isaia, V. Lippolis, G. L. Abbati, A. C. Fabretti, *Z. Anorg. Allg. Chem.* **2000**, *626*, 1454−1459. [9b] G. L. Abbati, M. C. Aragoni, M. Arca, F. A. Devillanova, A. C. Fabretti, A. Garau, F. Isaia, V. Lippolis, G. Verani, *Dalton Trans.* **2003**, 1515−1519.

[10] W. Kaim, B. Schwedersky, *Bioinorganic Chemistry: Inorganic Elements in the Chemistry of Life, an introduction and Guide*, Wiley-Interscience, New York **1991**, chapter 17, p. 338−343.

[11] H. G. Seiler, H. Sigel, A. Sigel, *Handbook on Toxicity of Inorganic Compounds*, Marcel Dekker, Inc., New York and Basel, **1988**, chapter 35, p. 419−436.

[12] The largest source of recycled mercury-containing products is the spent catalysts used in the production of chlorine and caustic soda, followed by electrical apparatus, dental amalgams, batteries, and other instruments such as thermometers. See: L. G. Twidwell, R. J. Thompson, *JOM-J. Miner. Met. Mater. Soc.* **2001**, *53*, 15−17.

[13] K. F. Purcell, J. C. Kotz, *Inorganic Chemistry*, W. B. Saunders Company, **1977**, chapter 5, p. 209−212.

[14] [14a] V. Garcia-Montalvo, J. Novosad, P. Kilian, A. M. Z. Slawin, P. Garcia y Garcia, M. Lopez-Cardoso, G. Espinosa-Perez, R. Cea-Olivares, *J. Chem. Soc., Dalton Trans.* **1997**, 1025−1029. [14b] O. Bumbu, A. Silvestru, C. Silvestru, J. E. Drake, M. B. Hursthouse, M. E. Light, *J. Organomet. Chem.* **2003**, *687*, 118−124. [14c] D. J. Crouch, P. M. Hatton, M. Helliwell, P. O'Brien, J. Raftery, *Dalton Trans.* **2003**, 2761−2766.

[15] S. Husebye, K. Maartmann-Moe, *Acta Chem. Scand., Ser. A* **1983**, *37*, 439−441.

[16] M. L. Delwaulle, *Bull. Soc. Chim. Fr.* **1955**, *247*, 1294−1299.

[17] [17a] M. C. Aragoni, M. Arca, C. Denotti, F. A. Devillanova, E. Grigiotti, F. Isaia, F. Laschi, V. Lippolis, L. Pala, A. M. Z. Slawin, P. Zanello, J. D. Woollins, *Eur. J. Inorg. Chem.* **2003**, 1291−1295. [17b] M. C. Aragoni, M. Arca, F. Demartin, F. A. Devillanova, F. Isaia, F. Lelj, V. Lippolis, A. Mancini, L. Pala, *Eur. J. Inorg. Chem.* **2004**, 3099−3109.

[18] C. Adamo, V. Barone, *J. Chem. Phys.* **1998**, *108*, 664−675.

[19] [19a] A. D. Becke, *J. Chem. Phys.* **1993**, *98*, 1372−1377. [19b] A. D. Becke, *J. Chem. Phys.* **1993**, *98*, 5648−5652. [19c] C. Lee, W. Yang, R. G. Parr, *Phys. Rev. B* **1988**, *37*, 785−789.

[20] A. Schafer, H. Horn, R. Ahlrichs, *J. Chem. Phys.* **1992**, *97*, 2571−2577.

[21] [21a] W. J. Stevens, M. Krauss, H. Basch, P. G. Jasien, *Can. J. Chem.* **1992**, *70*, 612−630. [21b] T.R. Cundari, W. J. Stevens, *J. Chem. Phys.* **1993**, 5555−5565.

[22] Basis sets were obtained from the Extensible Computational Chemistry Environment Basis Set Database, Version 6/19/03, as developed and distributed by the Molecular Science Computing Facility, Environmental and Molecular Sciences Laboratory which is part of the Pacific Northwest Laboratory, P.O. Box 999, Richland, Washington 99352, USA, and funded by the U.S. Department of Energy. The Pacific Northwest Laboratory is a multi-program laboratory operated by Battelle Memorial Institute for the U.S. Department of Energy under contract DE-AC06−76RLO 1830.

[23] The same calculation on **4** has also been performed with the larger Stuttgart RLC ECP basis set for the mercury atom. The calculated molecular orbital composition as well as the geometrical features are very close to those calculated with the SBKJC ECP basis set. Calculated Hg−S distances: 2.583, 2.564, 2.637, and 2.666 Å.

[24] R. Hoffmann, W. N. Lipscomb, *J. Chem. Phys.* **1962**, *36*, 2179−2189.

[25] A. Schmidpeter, R. H. Bohm, H. Groenger, *Angew. Chem.* **1964**, *76*, 860−861.

[26] SADABS Area-Detector Absorption Correction Program, Bruker AXS, Inc. Madison, WI, USA (2000).

[27] SHELXS-97; G. M. Sheldrick, *Acta Crystallogr., Sect. A* **1990**, *46*, 467−473.

[28] G. M. Sheldrick, SHELXL-97, *Program for Crystal Structure Refinement*, Universität Göttingen, Germany, **1997**.

[29] A. L. Spek, *Acta Crystallogr., Sect. A* **1990**, *46*, supplement C34, MS-02.01.05.

[30] M. J. Frisch, G. W. Trucks, H. B. Schlegel, G. E. Scuseria, M. A. Robb, J. R. Cheeseman, V. G. Zakrzewski, J. A. Montgomery, R. E. Stratmann, J. C. Burant, S. Dapprich, J. M. Millam, A. D. Daniels, K. N. Kudin, M. C. Strain, O. Farkas, J. Tomasi, V. Barone, M. Cossi, R. Cammi, B. Mennucci, C. Pomelli, C. Adamo, S. Clifford, J. Ochterski, G. A. Petersson, P. Y. Ayala, Q. Cui, K. Morokuma, D. K. Malick, A. D. Rabuck, K. Raghavachari, J. B. Foresman, J. Cioslowski, J. V. Ortiz, B. B.

Stefanov, G. Liu, A. Liashenko, P. Piskorz, I. Komaromi, R. Gomperts, R. L. Martin, D. J. Fox, T. Keith, M. A. Al-Laham, C. Y. Peng, A. Nanayakkara, C. Gonzalez, M. Challacombe, P. M. W. Gill, B. G. Johnson, W. Chen, M. W. Wong, J. L. Andres, M. Head-Gordon, E. S. Replogle, J. A. Pople, GAUSSIAN 98 (Revision A 11), Gaussian, Inc., Pittsburgh, PA, **1998**.
[31] [31a] W. Kuechle, M. Dolg, H. Stoll, H. Preuss, *Mol. Phys.* **1991**, *74*, 1245−1263. [31b] A. E. Reed, L. A. Curtiss, F. Weinholt, *Chem. Rev.* **1988**, *88*, 899−926.
[32] [32a] MOLEKEL 4.3, P. Flükiger, H.P. Lüthi, S. Portmann, J. Weber, Swiss Center for Scientific Computing, Manno (Switzerland), **2000**. [32b] G. Schaftenaar, J. H. Noordik, MOLDEN 3.6: a pre- and post-processing program for molecular and electronic structures, *J. Comp.-Aided Mol. Design* **2000**, *14*, 123−124. [32c] C. Mealli, D. M. Proserpio, *J. Chem. Educ.* **1990**, *67*, 399−402. [32d] R. Hoffmann, *J. Chem. Phys.* **1963**, *39*, 1397−1412.

Received April 5, 2004
Early View Article
Published Online October 18, 2004

